



Journal of Materials and Engineering Structures

Research Paper

Non-linear finite element investigation on the behavior of cold-formed plain lipped C-section in shear, and combined bending and shear

Tabassum Mahzabeen Raka *, Khan Mahmud Amanat

Department of Civil Engineering, Bangladesh University of Engineering and Technology, Dhaka 1000, Bangladesh

ARTICLE INFO

Article history:

Received : 30 May 2018

Revised : 27 July 2018

Accepted : 28 July 2018

Keywords:

Cold Formed

Effective Width Method

Finite Element Method

Shear Test

ABSTRACT

The paper provides numerical simulations, based on the finite element method (FEM) using the software package ANSYS/Standard, of high strength C-section cold-formed steel purlins in shear and combined bending and shear. The simulations were compared with the previous research on a variety of section sizes and thicknesses. The reasonable results of the numerical simulations show that finite element analysis can be used to predict the ultimate loads of thin-walled members including the post-buckling behavior of thin-walled sections in shear and combined bending and shear. It reveals that finite element analysis can therefore be used to design and optimize thin-walled sections of high strength steel. Direct Strength Method (DSM) design rules for C-sections in shear and for combined bending and shear both with and without tension field action can be investigated using this FE model.

1 Introduction

The advantages of using cold-formed steel material in constructions are very promising, which especially includes high strength to weight ratio, ease of construction and flexibility in fabrication. In addition, the cold-formed steel materials are generally fabricated in shapes of Z-sections, C-channel sections, hat sections and some other open sections, which are mainly produced by either brake-pressing or cold rolling techniques [1]. In both of the Australian standard and American specification for the design of cold-formed steel structures, which includes the developed direct strength method (DSM) of design and that was limited to pure compression and pure bending [2 - 4]. In addition, the DSM was mainly included in the North American Design Specification and in the Australian/New Zealand Standard more than a decade ago by considering as an alternative to the traditional effective width method (EWM) [4, 5]. One of the advantages of the DSM is that it estimates the structural capacities (e.g., bending, shear) without considering the calculation of cumbersome effective sections, especially with intermediate stiffeners. The development of the DSM for columns and beams, including the reliability of the method, has

* Corresponding author. Tel.: +61469804892.

E-mail address: raka12.c.e@gmail.com

already been investigated. To apply the DSM to purlin systems for shear and for combined bending and shear, vacuum rig tests on continuous lapped cold-formed purlins were applied to calibrate DSM design proposals for shear and combined bending and shear [6]. In addition, the experimental investigations were focused mainly on three different test series in which predominantly shear V , combined bending and shear MV and bending only M tests were performed [7]. In the study, two different section depths (150 and 200 mm) and three different thicknesses (1.5, 1.9 and 2.4 mm) of lipped channel sections were tested. Furthermore, in the investigation, tests with and without torsion/distortion restraint straps screwed on the top flanges adjacent to the loading points were also considered [8].

This paper concentrates numerical non-linear simulation, based on the finite element method (FEM) using the software package ANSYS, of plain C-section (cold-formed steel purlins) in shear, combined bending and shear, and bending only. However, the FE model was verified by using the experimental data conducted by Pham [7]. The model was developed by considering both of the material and geometric non-linearities. Large deflection effects were included in the FE model, thus stress stiffening effects were also included automatically in the FE model. This is how the FE model generated by ANSYS possessed the geometric non-linearity. Bilinear Kinematic Hardening property was applied in the material's nonlinearity to develop the FE model. The developed FE model was used to study the structural behaviour of the cold-formed purlins in shear, combined bending and shear, and bending only. In addition, plastic strain was included in order to obtain realistic models for the finite element nonlinear analysis. The developed FE model might be used for further investigation since it demonstrates the behaviour of purlin in shear and in combined bending and shear.

2 Finite Element Modeling of plain C-Section

2.1 Section Modelling

Fig. 1 illustrates the experimental and numerical cross section of the cold formed plain lipped C-section. The C-section was generalized to minimize the complexity of the FE model in which curved corner was simulated as straight line (Fig. 1a).

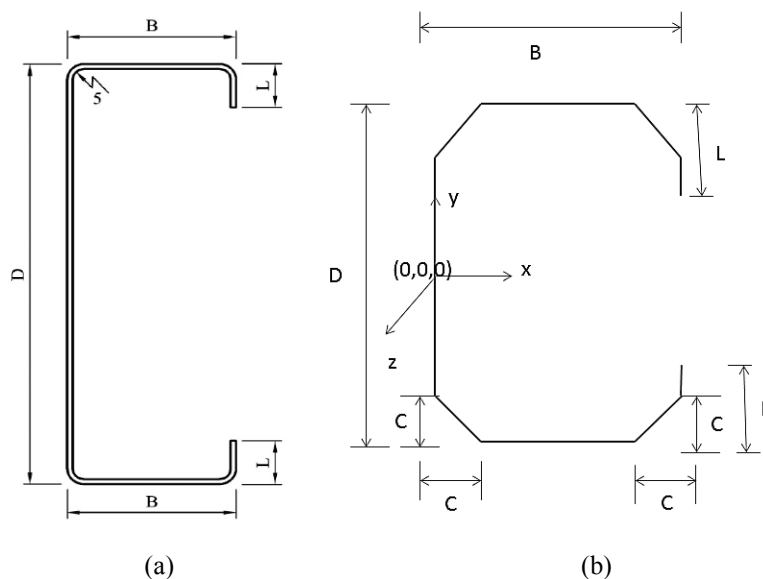


Fig. 1 –Cross-sectional parameters of plain C- section: (a) tested by Pham [7] and (b) FE model

2.2 Element modelling

In ANSYS, Shell elements are the type of elements that are suitable to efficiently model thin structures. Since this study concentrates on thin structural sections, shell element is the best option to get resemblance with the practical one. Therefore, SHELL181 was used for the model generation.

2.3 Material modelling(Nonlinear material properties: BKIN in ANSYS)

Cold-formed steel displays linear behaviour until the load exceeds the yield load, then the material shows large deformation which is no longer fully recoverable. The material behaviour can be described by a bilinear total stress-total strain curve starting at the origin and with positive stress-strain values. In order to obtain realistic models, for the finite element non-linear analysis, plastic strains are included. The plastic strain data of the sections was obtained from the experimental results found by Pham [7]. In FE model, the material non-linearity was incorporated by BKIN command. This command allows bilinear kinematic hardening behaviour of the material. Fig. 2 illustrates the bilinear kinematic hardening behaviour. As shown in the Fig.2, the initial slope of the curve is the elastic modulus (young modulus) of the material and beyond the user specified initial yield stress σ_0 , plastic strain develops and the back stress evolves so that stress versus total strain continues along a line with slope defined by the user specified tangent modulus E_T . This tangent modulus cannot be less than zero or greater than the elastic modulus E . For uniaxial tension followed by uniaxial compression, the magnitude of the compressive yield stress decreases as the tensile yield stress increases so that the magnitude of the elastic range is always $2\sigma_0$, as shown in this Fig. 2 [9].

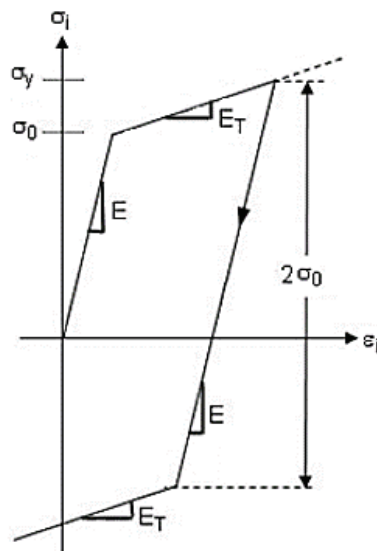


Fig. 2 –Stress vs. Total Strain for Bilinear Kinematic Hardening

2.4 Meshing

Normally, fine meshing leads to better results at the expense of greater simulation time, whereas coarse meshing results in lesser solution times and thus result accuracy might be compromised. Therefore, it is important to apply the mesh density for better solution accuracy without excess computation cost. An optimal solution is to use a fine mesh in areas of high stress gradient and a coarser mesh in the remaining areas. Pham [10] reported a mesh density analysis and found that 10×10 mm square elements show optimum simulation results. Here, an effort was made to get that optimum element mesh for shear series (V-series), combined bending and shear series (MV-series) and only bending series (M-series). The final mesh density was chosen so that results are not affected due to further dense meshing.

2.5 Boundary conditions and load application

The nodes along depth excluding two lips at support were selected and then translation in X and Y direction and rotation in Y and Z direction were restrained at these nodes. The origin (0, 0, 0) was selected and the translation in Z direction of this node was kept restrained. The nodes along depth excluding two lips at loading points were selected and the translation in X direction and rotation in Y and Z direction were restrained at these nodes. A displacement in Y direction was applied at these nodes. These boundary conditions were same for shear test series (V-series), combined bending and shear test series (MV-series) and only bending moment test series (M-series). The nodes along width of flange excluding two corners were selected

at strap location and then the translations in X direction were restrained at these nodes. The displacements in Y direction of these nodes at any strap location were kept same by defining a set of coupled degrees of freedom in ANSYS. But in only bending moment test series the translation in X direction of nodes at strap location away from support and loading points were not kept restrained. Fig.3 and 4 outline the boundary conditions.

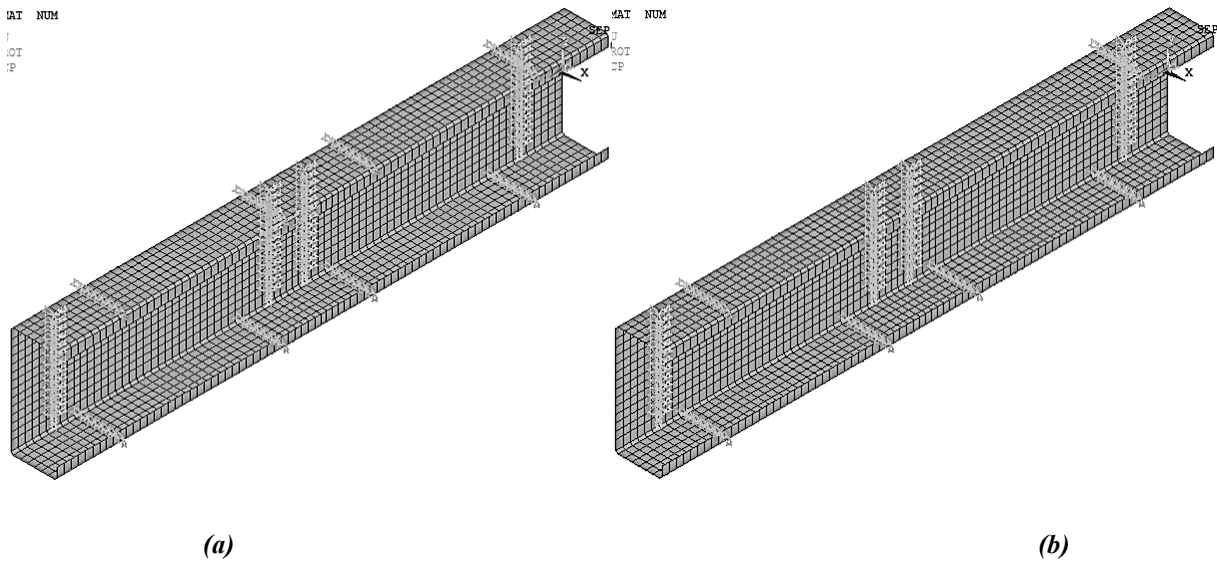


Fig. 3 –Boundary conditions and displacement application at nodes for shear test series (V-series) and combined bending and shear test series (MV-series): (a) with straps and (b) without straps

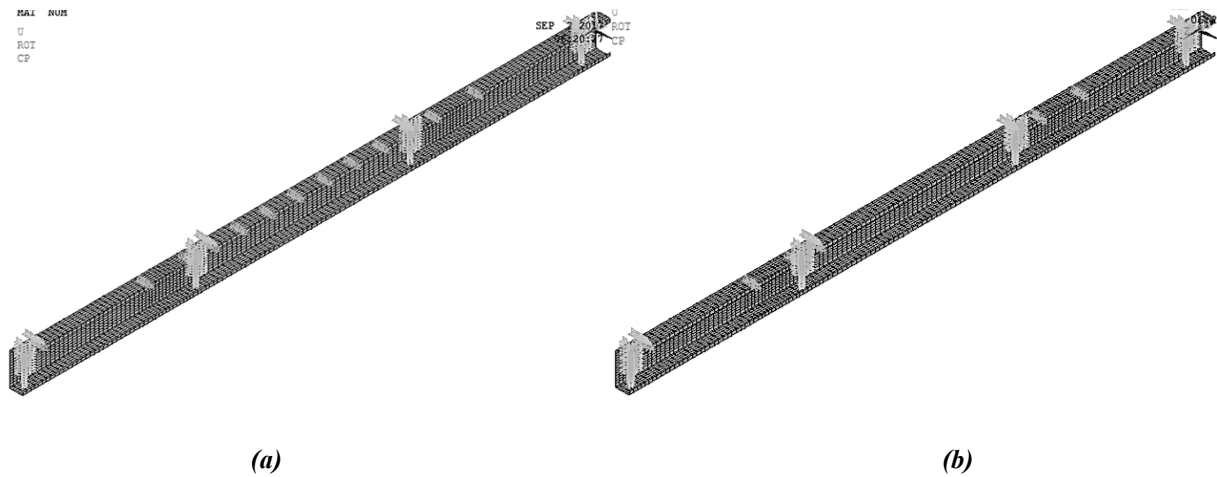


Fig. 4 –Boundary conditions and load application at nodes for only Bending moment test series (M-series): (a) with straps and (b) without straps

3 Verification of deformed shapes

The cold-formed sections are usually thinner than hot-rolled. With the resulting reduction of thicknesses of high strength steel, the failure modes of such sections are mainly due to instabilities such as local, distortional and flexural-torsional buckling modes or the interaction between them. The deformed shape of the FE model was compared with the physical model experiments conducted by Pham [7]. Fig.5 illustrates that the FE model develops diagonal tension field action just like the experimental one in shear test with straps for specimen C20019 [7]. Fig. 6 to 10 show the comparison between the deformed shapes that are found from FE model against the experimental models. These figures demonstrate that the buckling behaviour

of FE models is quite similar to that of the experimental model. This FE model can represent the physical system of the experimental model [7]. After comparison, it can be concluded that the buckling phenomena associated with the thin cold-formed members can be predicted successfully. This FE model might be used to study the buckling phenomena associated with the thin cold-formed members in shear test series, combined bending moment and shear test series and only bending test series.

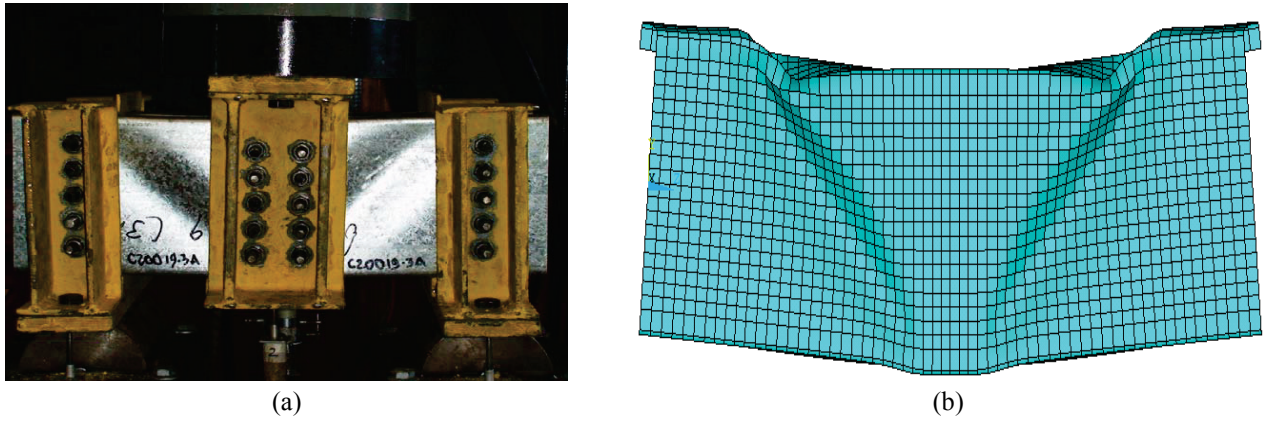


Fig. 5 –Buckling Mode Shape of V-C20019-With Straps: (a) tested by Pham [7] and (b) FEM model

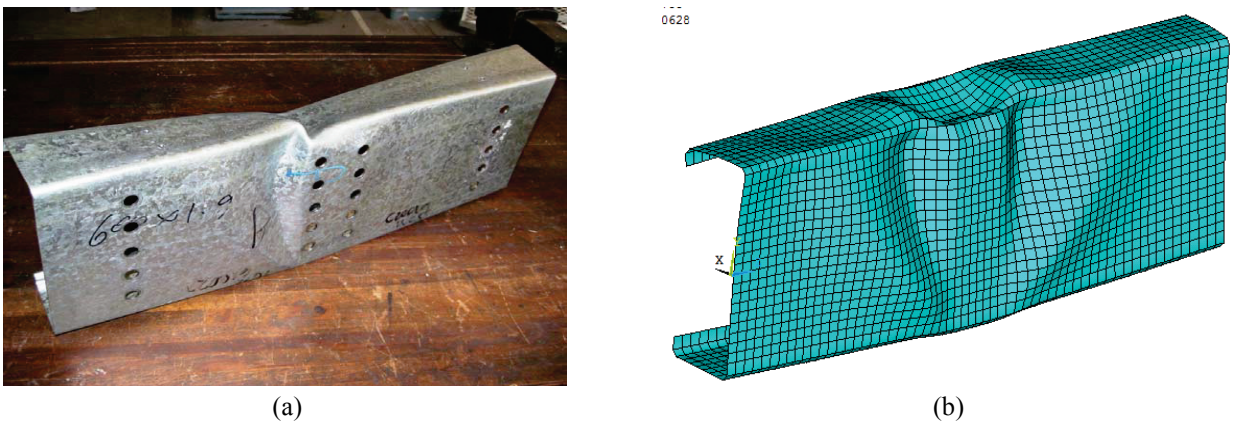


Fig. 6 –Buckling Mode Shape of V-C20019w-Without Straps: (a) experimented by Pham [7] and (b) FEM model

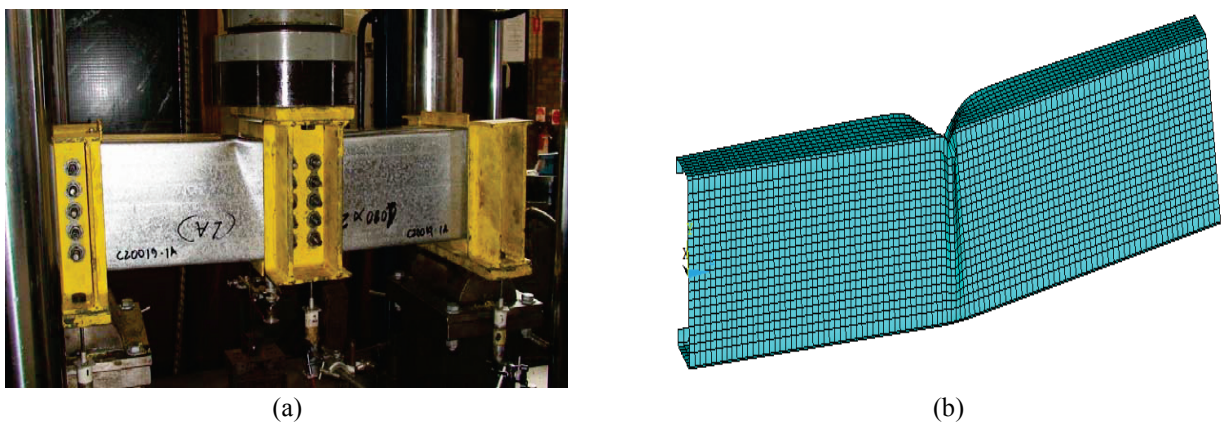
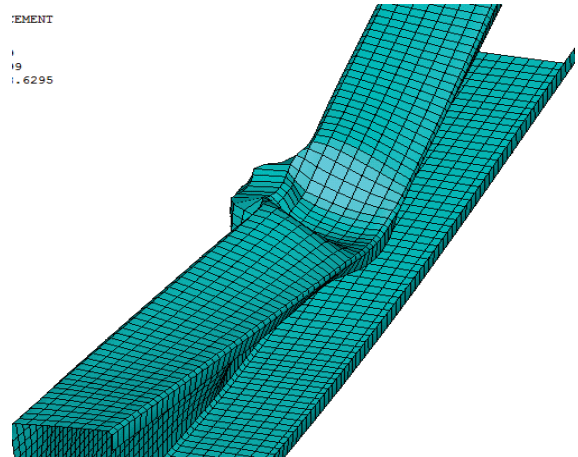


Fig. 7 –Buckling Mode Shape of MV-C20019-With Straps: (a) Physical model test by Pham [7] and (b) Numerical model



(a)

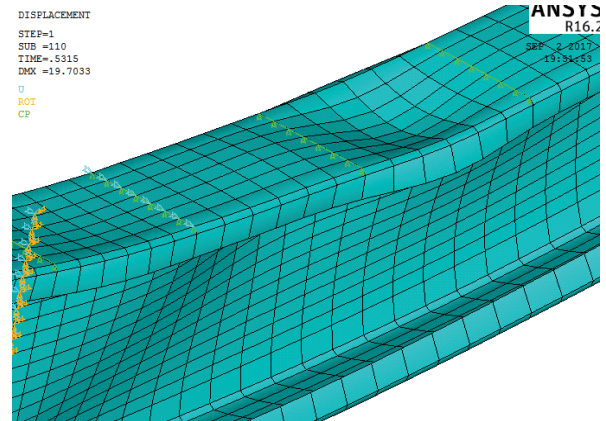


(b)

Fig. 8–Buckling Mode Shape of MV-C20019w-Without Straps: (a) experimental model by Pham [7] and (b) FEM model



(a)

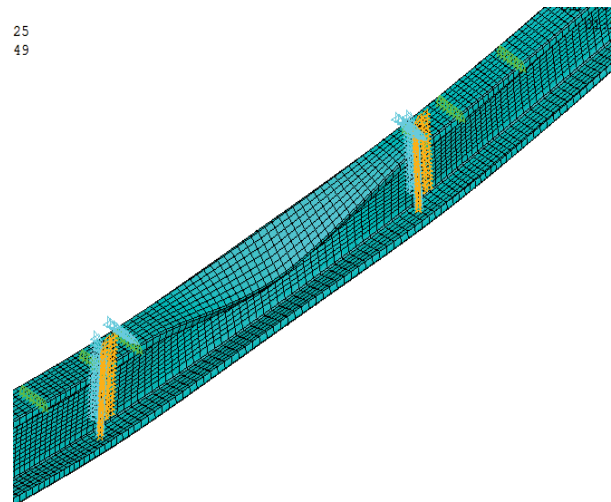


(b)

Fig. 9 –Failure Mode Shapes of M-C20019-With straps: (a) experimental model by Pham [7] and (b) FE model



(a)



(b)

Fig. 10 –Failure Mode Shapes of M-C20019w- Without Straps: (a) experimental model by Pham [7] and (b) FE model

4 Verification of the load - vertical displacement behaviour

For the verification of the FE model, the load-displacement (stiffness) behaviour of the FE model is compared with the experimental results found by Pham [7]. Table 1 outlines the specimen dimension and properties of Plain C-sections used by Pham [7]. Figs. 11 to 12 show that the slope of the line found from FE model, is much higher than that found by Pham [7]. It is found that the FE model can predict peak loads - maximum capacity of the sections. It is interesting that the stiffness of the FE model is much higher than that found experimentally by Pham [7]. This might happen due to the limitation in model generation. In the experimental set up, the test two beam specimens (C-section) were bolted together by M12 high tensile bolts at the supports and loading points as illustrated in Figs. 5a and 7a. However, in the case of FE model generation only one beam was simulated due to the structural symmetry and to minimize computation time. In addition, instead of modeling the bolts, boundary conditions were directly applied at the location of bolts along web. For this purpose in the FE model, the nodes along depth excluding two lips were selected at the supports and loading locations to apply the boundary conditions. Hence, this could be the reason of showing higher stiffness in the numerical simulation.

Table 1-Dimension and property specimen of test by Pham [7]

Test series	Section	Thickness (mm)	Depth (D) (mm)	Width (B) (mm)	Lip (L) (mm)	Yield stress (fy) (MPa)
V1	C15015	1.5	153.39	64.78	15.68	541.13
Vw	C15015	1.5	153.22	64.64	15.48	541.13
MV1	C15015	1.5	153.25	64.27	15.95	541.13
MVw	C15015	1.5	153.38	64.38	15.92	541.13
M1	C15015	1.5	153.46	64.53	15.02	541.13
Mw	C15015	1.5	152.7	64.77	16.51	541.13

Note: V1 and M1 refer to pure shear and bending with straps whereas Vw and Mw indicate shear and bending without straps; MV represents combined shear and bending. In section labelling, first three digit identify the web depth of the channel section and last two digit represent 10 times of channel thickness.

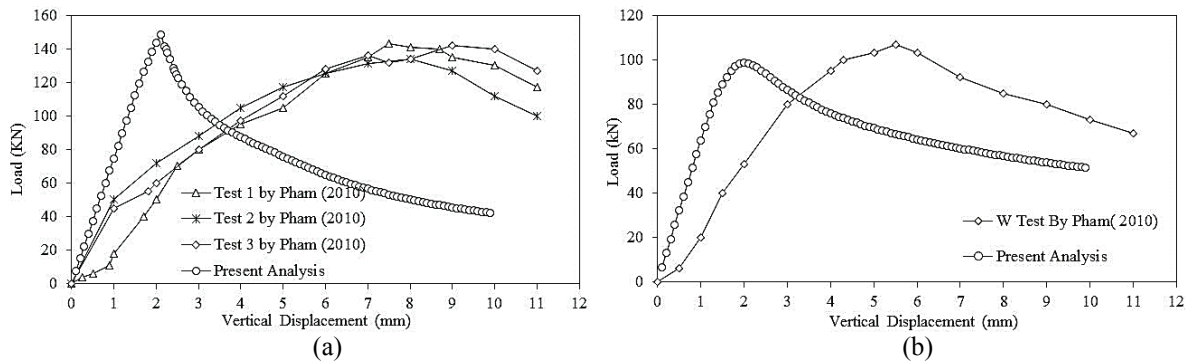


Fig. 11 – Load and Vertical Displacement Relations of MV-C15015: (a) with straps and (b) without straps

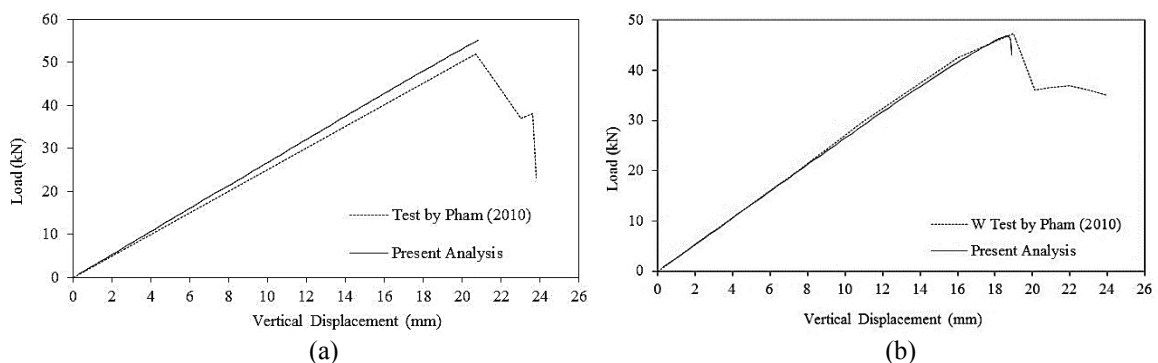


Fig. 12 – Load and Vertical Displacement Relations of M-C15015: (a) with straps and (b) without straps

5 Verification of peak loads

Figs. 13 to 15 compare the results of numerical simulation against the experimental results conducted by Pham [7]. Figs. 13a and 13b illustrate the variation of peak load for shear series with and without straps respectively. From the Fig.13a it is seen that the peak load found from numerical analysis is approximately 2.9% lower than that obtained from the experimental investigation for shear series (*V*) with straps. Similarly, in the case of shear series without straps, the difference of ultimate load capacity between numerical and experimental is about 6.49%, which is slightly higher than that found from with straps condition (Fig.13a). In the case of combined bending and shear series (*MV*), the similar trend of peak load variation is observed like as only shear series, and the difference of peak load between experimental and numerical is 3.5% and 7.8% with straps and without straps condition respectively (Figs. 14a and 14b). However, in the case of only bending series (*M*), the peak load found from the numerical analysis is approximately 5.5% higher than that evaluated from the experimental tests (Fig.15a), whereas the peak load capacity found from numerical and experimental analysis for without strap condition is almost equal – only 0.5% difference in loading capacity. Therefore, it could be concluded that the generated FE model might represent the physical model well.

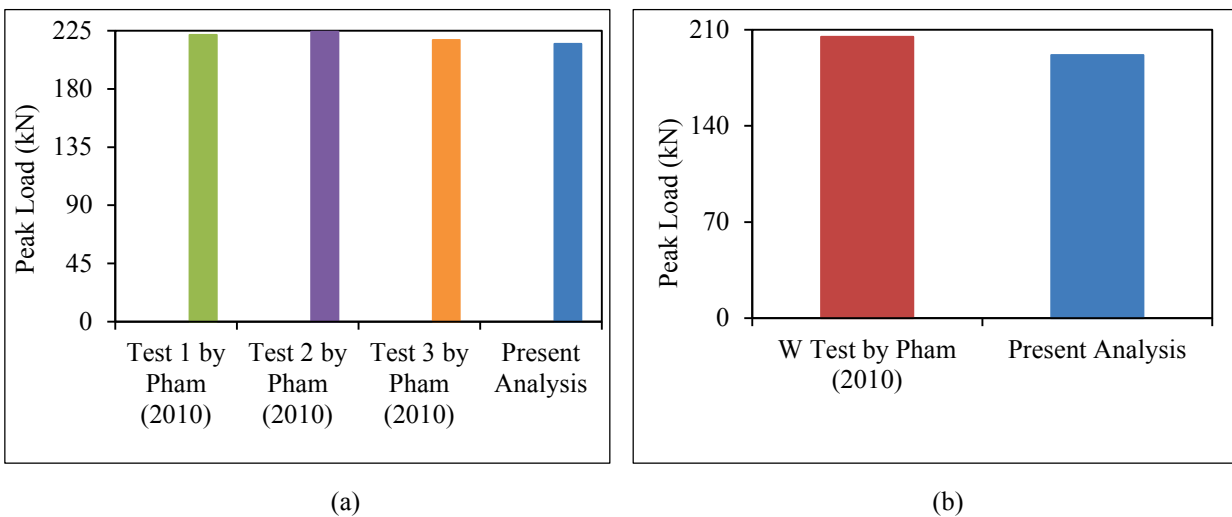


Fig. 13 –Peak loads found from various analysis *V-C15015*: (a) with straps and (b) without straps

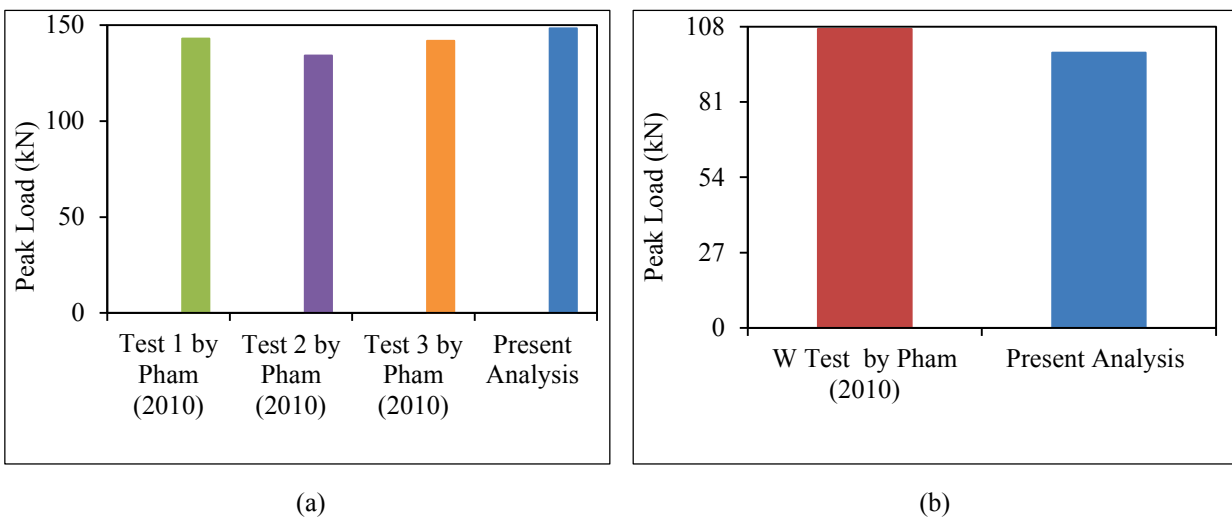


Fig. 14 –Peak loads found from various analysis *MV-C15015*: (a) with straps and (b) without straps

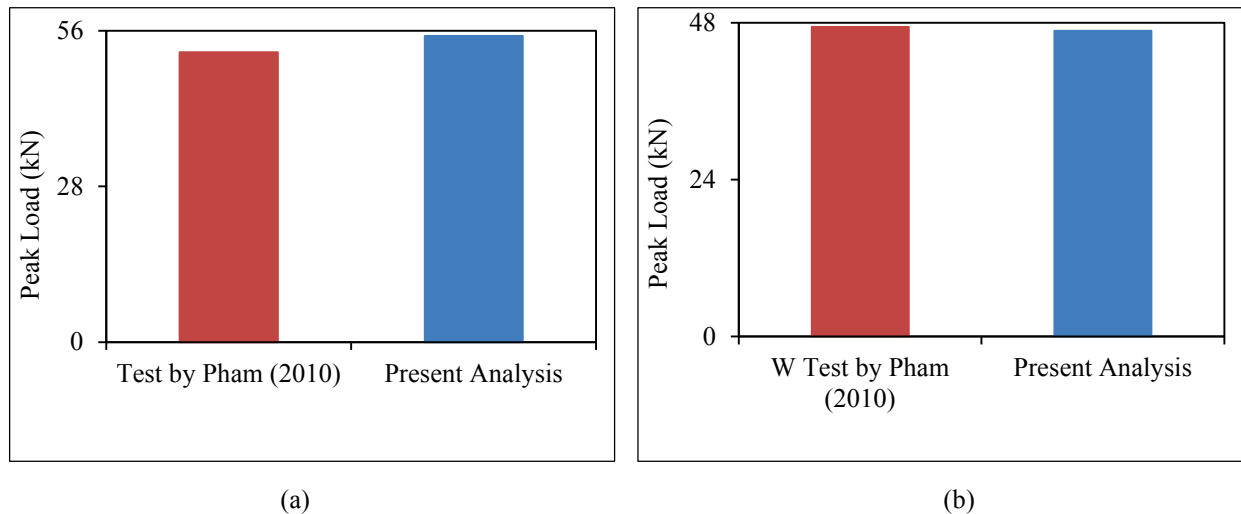


Fig. 15 –Peak loads found from various analysis M-C15015:(a) with straps and (b) without straps

6 Conclusion

In this study, a FE model was developed to study the structural behaviour of high strength cold-formed section in shear, combined bending and shear, and bending only, and the verification of the finite element model was done against the physical model experiment, which showed that FE model is in good agreement. From the numerical analysis, it is found that the FE models experience similar deflection patterns as found from the physical model study under different test series. In addition, the numerical model might also evaluate the peak load, which could be taken as the ultimate capacity of the plain lipped C-section. The peak loads found from the numerical analysis for shear, combined bending and shear, and bending differ only from 0.5% to 7.8% compared to the experimental results under different straps conditions. Hence, it might be outlined that the FE model could be used for further numerical study instead of performing extensive experimental research works.

REFERENCES

- [1]- I. Faridmehr, M.H. Osman, M.M. Tahir, M. Azimi, M. Gholami, Behaviour and design of cold-formed steel C-sections with cover plates under bending. *Int. J. Steel Struct.* 16(2016) 587-600. doi:10.1007/s13296-016-6026-9.
- [2]- NZS 4600:2005, Cold-formed steel structures, Australian/New Zealand Standard, Second edition, 2005
- [3]- AISI, North American Specification for the Design of Cold-Formed Steel Structural Members. Mexico, 2007.
- [4]- C.H. Pham, G.J. Hancock, Direct strength design of cold-formed C-sections for shear and combined actions. *J. Struct. Eng.* 138 (6) (2012) 759-768. doi:10.1061/(ASCE)ST.1943-541X.0000510.
- [5]- B.W. Schafer, T. Peköz, Direct strength prediction of cold-formed steel members using numerical elastic buckling solutions, thin-walled structures, research and development. In: Proceedings of the Fourteen International Specialty Conference on Cold-Formed Steel Structures, St. Louis, 1998, pp. 1-8.
- [6]- C. H. Pham, G. J. Hancock, Direct strength design of cold- formed purlins. *J. Struct. Eng.* 135(3) (2009) 229-238. doi:10.1061/(ASCE)0733-9445(2009)135:3(229).
- [7]- C. H. Pham, Direct Strength Method (DSM) of Design of Cold-Formed Sections in Shear, and Combined Bending and Shear, PhD Thesis, University of Sydney, 2010.
- [8]- C. H. Pham, G. J. Hancock, Experimental Investigation of High Strength Cold-Formed C-Section in Combined Bending and Shear. Research Report No R894, University of Sydney, 2009.
- [9]- C. H. Pham, G. J. Hancock, Numerical simulation of high strength cold-formed purlins in combined bending and shear. *J. Constr. Steel Res.* 66 (10) (2010) 1205-1217. doi:10.1016/j.jcsr.2010.04.014
- [10]- ANSYS®, Academic Research Mechanical, Release 16.2, Help system, Bilinear Kinematic Hardening, ANSYS, Inc, USA.